Journal of Scientific & Industrial Research
Vol. 84, December 2025, pp. 1341-1354
DOI: 10.56042/jsir.v84i12.16637

An Energy Efficient Load Management in Solar Integrated Power Network using Novel Metaheuristic Optimization

Sampatirao Nanibabu, Shakila Baskaran* & Prakash Marimuthu

Department of Electrical and Electronics Engineering, National Institute of Technology Nagaland, Dimapur 797 103, Nagaland, India

Received 24 January 2025; revised 23 June 2025; accepted 21 December 2025

The increasing demand for power driven by rapid urbanization poses significant challenges to modern power systems. To ensure a sustainable and stable energy supply, adopting effective energy management and Demand Side Management (DSM) strategies is crucial. This study introduces a novel energy optimization framework that combines DSM with the Wolverine Optimization Algorithm enhanced by a Time-Varying Exponential Coefficient (WoOA-TVEC). The adaptive nature of the exponential coefficient enables a dynamic balance between exploration and exploitation, resulting in faster convergence and improved optimization results. The proposed framework, integrated with time-dependent cost functions for Economic Load Dispatch (ELD) that support DSM, optimizes generator operations while adhering to system constraints, aiming for substantial cost reductions and enhanced system stability. To manage the intermittency of renewable energy sources and dynamic load conditions, the algorithm uses normalized solar photovoltaic (PV) generation profiles and real-time load factors. This enables the optimization model to efficiently respond to temporal changes in generation and demand while maintaining overall energy balance. Benchmark testing on standard mathematical functions showed that WoOA-TVEC outperformed other metaheuristic algorithms, including WoOA, Particle Swarm Optimization (PSO), Genetic Algorithm (GA), and Butterfly Optimization Algorithm (BOA), in terms of convergence speed, robustness, and solution quality. For the DSM application on the IEEE 14-bus system, WoOA-TVEC was compared with PSO, demonstrating significant improvements in total generation cost reduction and peak load shaving. These results confirm the scalability and practical relevance of the proposed framework for smart grid environments with renewable energy integration.

Keywords: Demand side management, Economic load dispatch, Solar photovoltaic system, Time-varying exponential coefficient, Wolverine optimization algorithm

Introduction

As global energy consumption continues to rise due to population growth, urbanization, and the widespread adoption of energy-intensive technologies, effectively managing energy demand has become increasingly critical. Traditional power systems, designed to respond to demand by increasing supply, struggle to handle peak loads, resulting in inefficiencies, higher operational costs, and increased environmental impacts. Additionally, while renewable energy is key to sustainable development, its variability complicates demand management.[1]

To address these issues, utilities are adopting Demand Side Management (DSM) strategies, which focus on optimizing energy consumption rather than solely increasing supply. DSM encourages consumers to shift their energy use to off-peak hours and adopt energy-efficient behaviors, thereby reducing peak demand, improving grid stability, and lowering greenhouse gas emissions.[2] Advanced technologies such as smart meters, demand-response initiatives, and real-time monitoring tools have enhanced DSM implementation, allowing utilities to manage growing energy demand more sustainably.[3]

DSM involves actions, programs, and technologies designed to align consumer energy usage with the availability of supply. Its primary goal is to reduce peak demand, optimize energy use, and improve resource efficiency.[4] Unlike supply-side solutions, which add generation capacity, DSM modifies consumer behaviour and promotes energy efficiency to balance load profiles.DSM plays a crucial role in addressing growing energy demands, environmental concerns, and the integration of renewable energy. By reducing peak demand, DSM minimizes the need for additional infrastructure and lowers generation and distribution costs. It also supports energy efficiency, reduces emissions, and facilitates the integration of renewables like wind and solar power.[5]

The concept of DSM has been widely studied as a solution to modern power system challenges. As

*Author for Correspondence
E-mail: shakila@nitnagaland.ac.in

electricity demand rises and renewable energy integration increases, DSM is seen as essential for optimizing energy use, reducing costs, and stabilizing grids.[6] Early research focused on the DSM's economic and technical benefits, especially its potential to delay investments in generation and transmission. More recent studies explore advanced optimization techniques, smart grid technologies, and the integration of distributed energy resources to enhance system flexibility and resilience. This section reviews key DSM research, including hybrid optimization approaches, economic load dispatch, and unit commitment strategies, which are critical for successful demand-side management.

Bustos *et al*.[7] proposed an Energy Management System (EMS) incorporating demand-side management (DSM) for coordinating multiple microgrids connected to a main grid. Utilizing a two-level hierarchical control with model-based predictive controllers (MPC), the system optimizes energy use, reduces power variations, and minimizes imported power. The EMS outperforms traditional systems, reducing power supply losses and battery cycling, as validated by simulations conducted on three microgrids. This study introduces an Improved Sine Cosine Algorithm (ISCA) for DSM in Smart Urban Buildings (SUBs), optimizing energy usage, reducing peak-to-average ratio (PAR), costs, and emissions while ensuring user comfort. The ISCA outperforms the Grasshopper Optimization Algorithm (GOA) and performs well in unscheduled scenarios. A Moth-Flame Optimization model further enhances energy storage scheduling and capacity planning for grid-connected SUBs.[8] A two-level collaborative DSM framework is proposed for distributed energy systems under carbon emission quotas. Encouraging user participation in demand response, it optimizes air conditioner use across building types, improving system efficiency, reducing carbon emissions, and enhancing thermal comfort without compromising user satisfaction.[9]

The study presents the Enhanced Cheetah Optimizer Algorithm (ECOA) for dynamic economic dispatch (DED), addressing DSM, renewable energy integration, and pumped-storage hydroelectric units. ECOA enhances grid security, reduces operational costs, and improves efficiency, demonstrating better adaptability and reliability in microgrid management and power flow problems, outperforming traditional algorithms.[10] This research explores DSM as an economic strategy to reduce generation costs by shifting demand to off-peak hours. It analyses wind power models and implements an economic DSM strategy, optimizing two microgrid systems using a hybrid CSAJAYA algorithm. Results show a 3–5% reduction in generation costs with 20% DSM participation, outperforming other optimization methods.[11] An innovative DSM method for peer-to-peer (P2P) energy sharing is proposed, ensuring fair participation and low-cost electricity through a uniform pricing and energy allocation mechanism. The method reduces community costs, power fluctuations, and revenue inequality, enhancing grid stability and fairness in energy distribution, outperforming traditional P2P sharing methods.[12] This paper introduces a DSM approach for residential consumers, aiming to balance electricity costs and user satisfaction by classifying appliances and developing a multi-objective optimization problem. A hybrid meta-heuristic algorithm efficiently solves the problem, with case study results demonstrating its effectiveness in optimizing appliance scheduling.[13]

A bi-level programming approach is proposed for the optimal allocation of electric vehicle charging stations in conjunction with wind turbines. The method minimizes power loss, optimizes station profit, and accounts for uncertainties in wind power and energy prices. Results show reduced power loss, increased profit, and benefits from feeder reconfiguration, with cryptocurrency miners affecting profit but not power loss.[14] A machine learning-based strategy for smart energy management among residential consumers is proposed, classifying them based on peak demand using a Random Forest classifier. The method achieves 92.23% accuracy and efficiently adjusts power loads, reducing daily power deficits by 0.73%, balancing growing energy demands with minimal consumer stress.[15] Demand Response Programs (DRP) can be used to reduce system losses and improve voltage profiles in distribution networks.[16] By encouraging consumers to adjust their electricity use during peak hours, DRP reduces power losses and improves voltage profiles, benefiting both utilities and consumers, and thereby enhancing social welfare. A Hybrid Emperor Penguin Glowworm Swarm Optimization (EP-GSO) algorithm is introduced for microgrids, integrating renewable energy sources like wind, PV, and energy storage. The model optimizes energy supply costs, power loss, and voltage fluctuations. Results show superior performance in reducing voltage fluctuations compared to other optimization methods, enhancing microgrid stability.[17] Another study[18] proposes a stochastic framework for scheduling renewable-based microgrid systems, focusing on generation and demand-side flexibility. The tri-layer model minimizes operation costs, improves thermal and electrical flexibility, and optimizes DSM. The approach demonstrates a 22.98% improvement in electrical flexibility and a 34.64% improvement in thermal flexibility, as shown in the day-ahead results.

The existing literature on DSM highlights various approaches to optimize energy usage, reduce costs, and improve system efficiency. However, significant research gaps persist in developing comprehensive and adaptive solutions using novel meta-heuristic algorithms. While algorithms such as the Improved Sine Cosine Algorithm (ISCA), Enhanced Cheetah Optimizer Algorithm (ECOA), and hybrid methods like CSAJAYA and EP-GSO have shown promise, the exploration of newer, more robust, and scalable meta-heuristic algorithms remains limited. Most studies focus on either cost optimization or energy efficiency in isolation, with limited emphasis on solutions that address both objectives simultaneously. Additionally, existing methods, such as MPC and stochastic frameworks, lack the adaptability required for dynamic, real-time energy demands and market conditions.

To address these limitations, this study proposes the use of the Wolverine Optimization Algorithm (WoOA), a bio-inspired metaheuristic known for its aggressive yet strategic search dynamics, which is further enhanced through the addition of a Time-Varying Exponential Coefficient (TVEC). WoOA exhibits superior adaptability, maintaining an effective balance between exploration and exploitation, which is essential for solving complex, nonlinear, and constrained energy optimization problems. In contrast to conventional algorithms such as Particle Swarm Optimization (PSO), Genetic Algorithm (GA), and Butterfly Optimization Algorithm (BOA), WoOA demonstrates better convergence speed, stronger avoidance of local optima, and improved responsiveness to intermittent renewable generation and dynamic demand variations. By integrating TVEC, the WoOA-TVEC framework gains additional flexibility, allowing the search process to evolve intelligently over time to meet operational and environmental objectives. Integrating DSM with renewable energy sources has been explored, but a holistic approach that enhances cost-effectiveness, peak load reduction, and renewable penetration simultaneously remains underexplored. User-centric optimization, which balances user comfort, cost, and energy efficiency, is another area requiring attention. Furthermore, benchmarking against a wide range of optimization techniques is often inadequate. Addressing these gaps with the proposed WoOA-TVEC algorithm can provide an adaptive, scalable, and reliable solution for modern smart grid environments.

The main contributions of this article are as follows:

- This study incorporates DSM strategies into the IEEE 14-bus system with Time Varying Exponential Coefficient (TVEC) for energy optimization.
- The proposed WoOA-TVEC is benchmarked and tested against various optimization algorithms to evaluate its effectiveness and robustness.
- Economic Load Dispatch (ELD) with time-varying cost functions and Unit Commitment (UC) techniques are implemented to optimize generator operations, achieving significant cost savings and improved reliability.
- Solar photovoltaic (PV) systems are integrated and assessed using L-index calculations, ensuring enhanced voltage stability and improved system resilience.
- Detailed performance analyses highlight the superior effectiveness of the proposed methods in enhancing cost efficiency, system stability, and renewable energy integration.

Methodology

The IEEE 14-bus system shown in Fig. 1 is a standardized test system widely used in power system analysis for research, simulation, and validation of power flow, stability, and optimization studies.[19] It serves as a benchmark model for testing and computing various power system algorithms and techniques under specific conditions. The system represents a simplified model of a real-world power grid containing components such as buses, generators, loads, and transmission lines. The standard IEEE 14-bus system comprises 14 buses, five generators, 20 transmission lines, 11 loads, and three transformers. This system assumes a balanced three-phase operation, which simplifies the analysis.

In this study, DSM is distinctly treated as a load-side strategy aimed at shifting demand profiles to reduce peak loads and enhance load factor, without altering total energy consumption. In contrast, ELD and UC are modeled as supply-side mechanisms

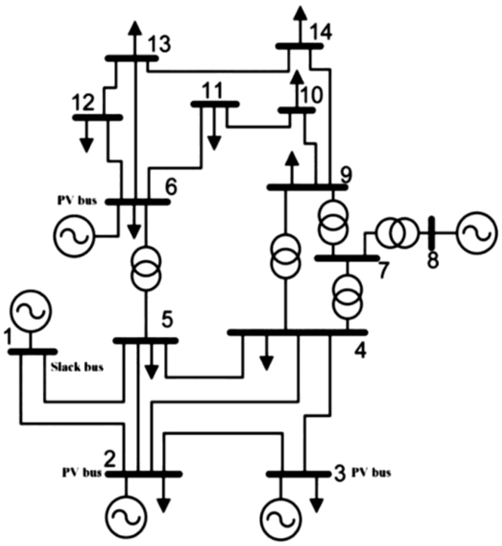

Fig. 1 — Standard IEEE 14 bus system

focused on optimal generator scheduling. To avoid ambiguity, DSM is applied as a preprocessing step, modifying the hourly demand vector prior to supply-side optimization. This separation ensures methodological clarity between consumer-end demand control and generator-side dispatch planning.

The primary objective of the proposed DSM application for the IEEE 14 bus system is to minimize the total energy cost while reducing the system's peak load consumption. This can be modeled mathematically as a minimization function, as shown in Eq. (1) below.

$$Minimise\ \sum_{t=1}^{T}\left(P_L(t) - P_{Obj}(t)\right)^2 \qquad \ldots (1)$$

where, $P_L(t)$ is the total actual power consumption during any time t, which is shown in Eq. (2) and $P_{Obj}(t)$ is the estimated power consumption during the DSM operation.

$$P_L(t) = \sum_{i=1}^{n} P_d(t) \qquad \ldots (2)$$

The total load is calculated as the sum of power consumption ($P_d(t)$) from each bus in the system. The objective power consumption is calculated by the objective function shown in Eq. (3)

$$P_{Obj}(t) = \frac{\sum_{t=1}^{24} P_g(t)}{C_T(t).P_{avg}} \qquad \ldots (3)$$

where, $P_g(t)$ is the power generated in the system at each time t, and P_{avg} is the average power production by all the generators. The total power generation ($P_G(t)$) in the system must satisfy the following constraint in Eq. (4).

$$P_G(t) = P_L(t) - P_{RE}(t) - P_{sh}(t) \qquad \ldots (4)$$

where, $P_{RE}(t)$ is the power generation from the renewable energy sources available from the system. $P_{sh}(t)$ is the amount of load that is scheduled to be delayed or operated is decided by DSM operation and it is negative if the load is scheduled to operate and is positive if it is delayed. The DSM program determines the value of $P_{sh}(t)$ based on the objectives. $P_{Obj}(t)$ value is decided by optimally allocating the generation among each generator using ELD problem.[20] ELD uses an incremental cost curve, which is different for each generator, to allot each generator with a specified generation for minimum cost of operation. In this study, the ELD formulation is employed as a tool to address the DSM problem. Transmission losses are neglected to simplify the optimization framework and to emphasize the core performance evaluation of the proposed WoOA-TVEC algorithm. The total cost of the power generation is calculated by using the following Eqs (5–7).

$$C_i(t) = \alpha_i P_{G_i}(t)^2 + \beta_i P_{G_i}(t) + \gamma_i\ {}^{\$}/_{h} \qquad \ldots (5)$$

$$C_T(t) = \left(\sum_{i=1}^{k} C_i\, P_{G_i}(t)\right) + {}^{C_{pv}}/_{hour}\ \$ \qquad \ldots (6)$$

$${}^{C_{pv}}/_{hour} = \frac{C_{inst}\cdot p}{365\times24\times y} + \frac{C_{o\&m}\cdot p}{365\times24} \qquad \ldots (7)$$

where, $C_i(t)$ is the cost of power generation of *i*th generator, α_i, β_i, γ_i are the cost coefficients of *i*th generator, $C_T(t)$ represents the total cost of electricity combined from all the sources, C_{pv} represents the cost of electricity generated through solar PV, C_{inst} represents the installation cost of the solar PV per kW capacity, $C_{o\&m}$ represents the operation and maintenance cost of the solar PV per kW capacity, p is the total power capacity of the solar PV, and y is the total life time of the solar PV.

Solar PV panels generally last 20 to 25 years. Factors that determine lifetime include material quality, installation techniques, ambient conditions, and adherence to maintenance routines. Solar panels lose efficiency over time due to deterioration. Most panels degrade at a rate of 0.5% to 1% each year, which means that they may retain 75% to 85% of their original capacity after 25 years. This article examines the critical values of the life span and maintenance costs in relation to real-time scenarios.

Line Stability Index

Voltage stability in power systems is fundamentally concerned with the system's ability to maintain acceptable voltage levels under normal conditions and following disturbances. The L-index serves as a scalar, bus-wise indicator of voltage stability, reflecting the degree of proximity to voltage collapse.[21] It is computed based on load flow solutions and the system's impedance matrix, taking into account the interaction between generation and load buses. The value of the L-index ranges from 0 (ideal stability) to 1 (voltage instability or collapse). As the system becomes more heavily loaded or reactive power margins are depleted, the L-index values at certain buses increase, indicating a reduction in voltage stability. A higher L-index at any load bus signifies increased sensitivity to voltage fluctuations, making that bus a potential vulnerability point in the network. In this study, the L-index was evaluated for all load buses, and the maximum L-index was used as a global indicator of the system's weakest voltage stability margin. A decrease in the maximum L-index after DSM application and PV integration suggests enhanced voltage support, improved reactive power distribution, and a more resilient operating point in terms of voltage collapse. Therefore, the L-index serves as a reliable and computationally efficient metric for quantifying and comparing voltage stability across different control strategies. The mathematical formula for calculating the L-index is presented in Eq. (8).

$$L_i = 1 - \sum_{j=1}^{n} \left| F_{ij} \right| \frac{V_j}{V_i} e^{j(\delta_j - \delta_i)} \quad \ldots (8)$$

where, i is the load bus, j is the generator bus, V_i and V_j are voltage magnitudes of load and generator buses, δ_i and δ_j are the voltage angles of the load and generator buses and F_{ij} is the element of the modified power flow Jacobian matrix that relates load and generator buses, as given in Eq. (9) below.

$$F_{ij} = -[Y_{LL}]^{-1} Y_{LG} \quad \ldots (9)$$

where, Y_{LL} is the submatrix corresponding to load buses and Y_{LG} represents the submatrix coupling load buses and generator buses. These equations calculate the line stability index for all buses in the IEEE 14-bus system, as shown in Table 1 below.

To improve the system's stability, a 5 MVA solar PV unit is integrated at the 14th bus. Given that the total apparent power demand at this bus is approximately 13.35 MVA, the PV penetration level is 37.45%. This bus was selected based on L-index sensitivity analysis, indicating it as one of the most voltage-stressed locations. The integration of PV at this point supports local load demands, reduces the burden on central generators, and enhances overall system stability and operational resilience. The normalized daily load profile and solar PV generation pattern used in this study were derived from publicly available real-time datasets[22] which reflect typical demand and irradiance trends applicable to grid-level simulation studies. The PV generation and normalized load curve for a 24-hour duration is shown in Fig. 2 below.

Load Profile

The normalized load curve, as shown in Fig. 2, is a vital analytical tool used in energy management and power system analysis. It provides a simplified representation of a consumer's energy consumption over time, allowing for more straightforward comparisons across different periods, user profiles, and energy management strategies.[23] The theory

Table1 — L-index of IEEE 14 bus system

Bus ID	L-index	Bus ID	L-index
Bus-1	0	Bus-8	0.5071
Bus-1	0	Bus-9	0.5476
Bus-3	0	Bus-10	0.6430
Bus-4	0.2965	Bus-11	0.7078
Bus-5	0.4218	Bus-12	0.7970
Bus-6	0	Bus-13	0.8278
Bus-7	0.1594	Bus-14	0.8757

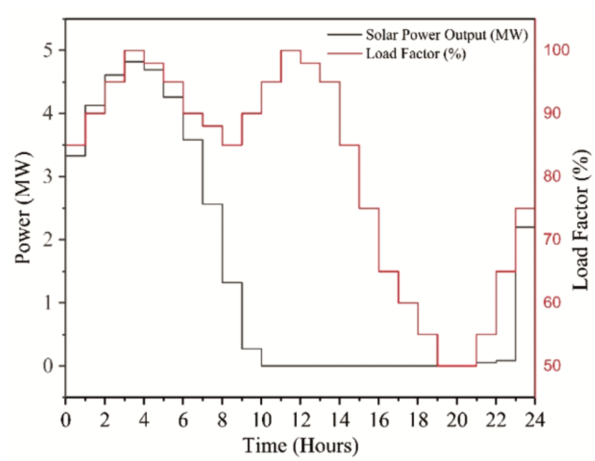

Fig. 2 — Solar PV data and aggregate load factor of a typical day (starting from 7:00 AM)

behind the normalized load curve is founded on standardizing power consumption data, making it independent of the absolute scale of energy use. This normalization process enables analysts to observe patterns in energy use, assess efficiency, and make informed decisions regarding demand-side management. Normalization involves adjusting the raw load data to create a uniform basis for comparison. This is typically achieved by dividing the actual load at each time interval by a reference load, which could be the peak load, average load, or the total energy consumed over a specific period. The formula for normalization can be expressed as shown in Eqs (10, 11) as follows:

$$P_d(t) = P_d^{base}.Load\ factor(t) \quad \dots (10)$$

$$Q_d(t) = Q_d^{base}.Load\ factor(t) \quad \dots (11)$$

where, $P_d(t)$ is the active power demand in the bus at time t, P_d^{base} represents the maximum active power demand before normalization, $Load\ factor(t)$ represents the normalized load factor value at time t, $Q_d(t)$ is the reactive power demand in the system at time t, Q_d^{base} represents the maximum reactive power demand before normalization. Normalized load curves can be analysed over various time frames, such as hourly, daily, weekly, monthly, or seasonally. This flexibility allows analysts to capture short-term fluctuations while also identifying long-term trends in consumption behaviour. Different consumer categories — residential, commercial, and industrial — display unique load profiles influenced by operational patterns and energy usage. By normalizing these load curves, analysts can compare different consumer types without the distortion of scale, highlighting differences in peak demand, usage patterns throughout the day, and seasonal variations. The normalized load curve serves as a benchmark for evaluating the effectiveness of energy management programs.

Wolverine Optimization Algorithm with Time Varying Exponential Coefficients (WoOA-TVEC)

The wolverine, the largest terrestrial species in the Mustelidae family, predominantly inhabits remote regions of the subarctic and alpine tundra and the northern boreal forests of the Northern Hemisphere.[24] Among the natural behaviours of wolverines in the wild, their feeding strategies stand out prominently. Wolverines employ two primary methods to feed: (i) scavenging and (ii) hunting. In scavenging, they locate carrion by tracking other predators and feeding on the remains. In hunting, they pursue live prey, chasing and fighting before ultimately killing and consuming it. These two feeding strategies demonstrate remarkable intelligence and have inspired the mathematical modelling to develop the proposed WoOA approach. At the beginning of the algorithm's execution, the initial placement of wolverines within the problem-solving space is randomized using Eq. (12).

$$x_{i,d} = lb_d + r(ub_d - lb_d) \quad \dots (12)$$

where, $x_{i,d}$ represents its value of position in the dth dimension of the search space, lb_d represents the lower bound of the dimension, ub_d represents the upper bound of the dimension, and r is the random number.

The Scavenging strategy of WoOA entails updating the positions of population members within the problem-solving space by emulating the wolverine's natural feeding behaviour on carrion. In this strategy, the wolverine tracks the paths of other predators to locate and feed on their leftover kills. Simulating the wolverine's movement in response to predator activity introduces a novel approach to exploring the solution space. In the WoOA framework, the positions of other members with superior objective function values are treated as the predators' locations, representing potential sources of leftover kills for each wolverine, as defined in Eq. (13).

$$CP_i = \{X_k : F_k < F_i\ and\ k \neq i\}, i = 1, 2, \dots, N\ and\ k \in \{i\} \quad \dots (13)$$

As the wolverine moves toward the chosen predator to reach the carrion, a new proposed position for the corresponding member is calculated using Eq. (14). A Time Varying Exponential Coefficient (TVEC) is introduced in the position updating equations for improving the exploration and exploitation phases. This new improved algorithm is named WoOA-TVEC. If this position results in an improved objective function value, it replaces the member's previous position as per Eq. (15).

$$x_{ij}^{S1} = x_{ij} + W_{S1}.r_{ij}.\left(SP_{ij} - I_{ij}.x_{ij}\right) \quad \dots (14)$$

$$X_i = \begin{cases} X_i^{S1}, F_I^{S1} \leq F_i \\ X_i, else \end{cases} \quad \dots (15)$$

where, CP_i represents the candidate predators' location set for each wolverine, X_k is the member in the population with a better objective function, F_k is the value of the objective function for X_k, F_i is the objective function of i[th] Wolverine, x_{ij}^{S1} is the updated position of the wolverine during the scavenging strategy, x_{ij} is the initial position of Wolverine, SP_{ij} represents the selected predator from the set CP_i, and X_i is the new updated position of Wolverine after completing the iteration, W_{S1} is the weight coefficient and is linearly decreasing throughout the iterations as shown in Eq. (16).

$$W_{S1} = \frac{W_{max} - W_{min}}{n} \quad \ldots (16)$$

where, W_{max} is a constant value and is equal to 0.8, W_{min} is equal to 0.2. The hunting strategy in WoOA-TVEC updates the positions of population members within the problem-solving space by emulating the wolverine's natural hunting behaviour. This process replicates the wolverine's approach to hunting, which involves attacking live prey, engaging in a chase and fight, and ultimately securing and feeding on the kill. Based on this strategy, the position update is divided into two phases: (i) exploration, which simulates the wolverine's movement toward the prey, and (ii) exploitation, which mimics the chase and fight between the wolverine and its prey.

During the attacking phase of WoOA-TVEC, the positions of the population within the problem-solving space are adjusted by simulating the wolverine's attack on its prey. By mimicking the wolverine's movements during a hunt, substantial changes are made to the population's positions, enhancing WoOA-TVEC's exploration capability in navigating the problem-solving space. The position of the wolverine updates according to Eqs (17, 18).

$$x_{ij}^{P1} = x_{ij} + W_{P1}.r_{ij}.(prey_j - I_{ij}.x_{ij}) \quad \ldots (17)$$

$$X_i = \begin{cases} X_i^{P1}, F_I^{P1} \le F_i \\ X_i, else \end{cases} \quad \ldots (18)$$

where, $prey_j$ is the best population member in j[th] dimension, x_{ij}^{P1} is the position of the member during the phase, F_I^{P1} represents the value of the objective function at the new location. The flowchart of the WoOA-TVEC is represented in Fig. 3.

During the fighting and chasing phase of WoOA-TVEC, the positions of population members in the problem-solving space are updated by simulating the

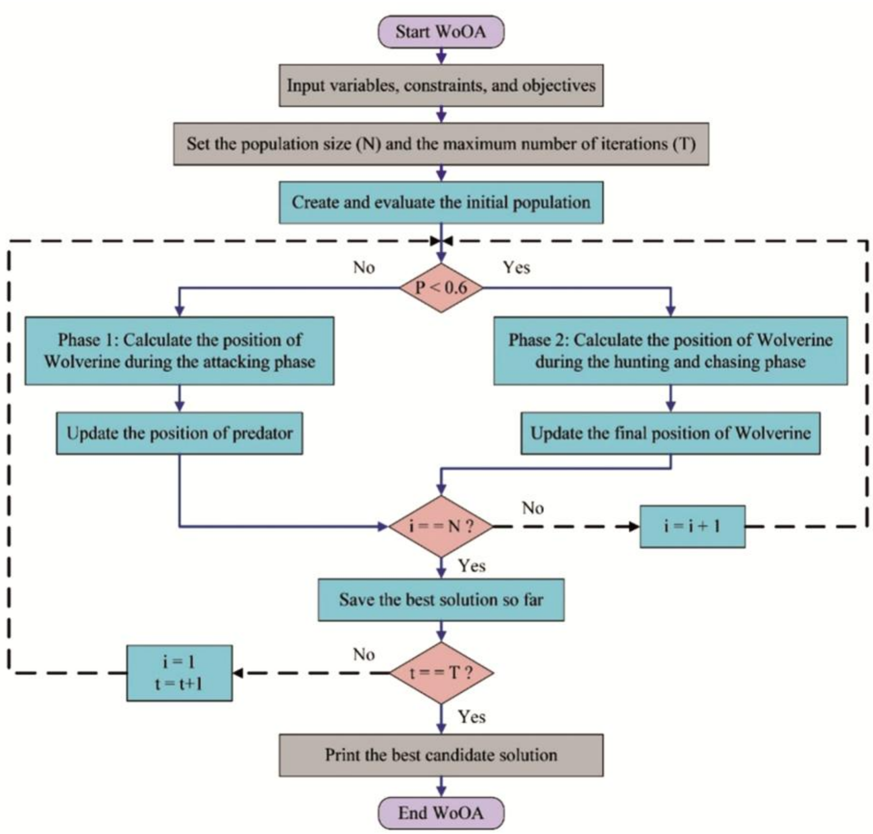

Fig. 3 — Flow chart of WoOA-TVEC

interactions between the wolverine and its prey during a hunt and pursuit. These simulated movements introduce minor adjustments to the population members' locations, enhancing WoOA-TVEC's local search capability within the problem-solving space. By modelling the wolverine's movements during the hunt and pursuit, a new position for each WoOA-TVEC member is calculated using Eq. (19). This new position leads to an improved objective function value, as described in Eq. (20).

$$x_{ij}^{P2} = x_{ij} + W_{P2}.\left(1 - 2r_{ij}\right).\frac{ub_j - lb_j}{t} \quad \ldots (19)$$

$$X_i = \begin{cases} X_i^{P2}, F_l^{P2} \le F_i \\ X_i, else \end{cases} \quad \ldots (20)$$

where, X_i^{P2} is the new position of i[th] wolverine determined based on the hunting and chasing phase, x_{ij}^{P2} represents the position of wolverine in j[th] dimension, W_{P1}, W_{P2} are the weight factors coefficients which are equal and follows the Eq. (21).

$$W_{P1} = W_{P2} = 1 - \frac{1}{e^{\frac{1}{n}}} \quad \ldots (21)$$

The time-varying exponential coefficient used in the proposed WOA-TVEC algorithm is not arbitrarily selected; it is conceptually grounded in adaptive control and dynamic parameter tuning principles. This specific function offers a smooth and bounded transition, effectively balancing exploration and exploitation. In early iterations, the lower coefficient value promotes broad search across the solution space, supporting global exploration. As iterations progress, the coefficient gradually increases, focusing the search on promising regions to enhance local exploitation. This gradual modulation mitigates the risk of premature convergence and improves solution quality compared to conventional metaheuristic algorithms.

Table 2 presents the results from the WoOA-TVEC, WoOA, BOA, GA, and PSO algorithms, along with a comparison of the mean and standard deviation values for each benchmark function[25] across 30 runs. To ensure a comprehensive validation of the algorithm's superiority, a diverse suite of benchmark

Table 2 — Comparison of proposed WoOA-TVEC with different algorithms;
(BOA: Butterfly Optimization Algorithm, GA: Genetic Algorithm), Rank: Wilcoxon rank test results

Function	Confidence Interval		WoOA-TVEC	WoOA	BOA	GA	PSO
f_1	[–100, 100]	Mean	0	0	0	2.2039E-02	1.7665E-51
		SD	0	0	0	9.6789E-03	1.1246E-50
		Rank	1	1	1	3	2
f_2	[–4.5, 4.5]	Mean	0	1.9862E-04	0	0	0
		SD	0	3.1284E-04	0	0	0
		Rank	1	2	1	1	1
f_3	[–100, 100]	Mean	0	0	0	2.1954E-04	3.1041E-53
		SD	0	0	0	1.0961E-04	2.1065E-52
		Rank	1	1	1	3	2
f_4	[–100, 100]	Mean	0	2.2143E-01	0	2.3026E-02	1.3116E-31
		SD	0	4.8828E-01	0	1.0512E-02	6.653E-31
		Rank	1	4	1	3	2
f_5	[–1,281, 1.281]	Mean	4.98E-05	5.0968E-01	3.8917E-05	2.7387E-03	3.7408E+00
		SD	2.63E-05	1.3056E-01	2.9019E-05	8.5056E-04	1.0296E+00
		Rank	1	4	2	3	5
f_6	[–100, 100]	Mean	0	0	0	0	3.0393E-02
		SD	1.00E-15	0	0	0	2.6192E-17
		Rank	2	1	1	1	3
f_7	[–32, 32]	Mean	1.62E-01	3.5689E+00	1.7183E+00	4.6683E-02	1.8186E+01
		SD	8.60E-04	6.8939E-01	0	1.6847E-02	5.4812E+00
		Rank	2	3	3	1	4
f_8	[–600, 600	Mean	1.73E-19	5.4987E-01	1.8472E-19	5.5598E-02	4.0503E+01
		SD	1.77E-20	2.7198E-01	2.6886E-20	2.9490E-02	4.1334E+01
		Rank	1	4	2	3	5
f_9	[–10, 10]	Mean	3.18E-01	3.1092E-02	4.4108E-01	1.3732-04	4.9297E+00
		SD	2.65E-02	4.8193E-02	5.7467E-02	7.6553E-05	5.9951E+00
		Rank	3	2	4	1	5
f_{10}	[0, π]	Mean	−1.33E+00	−9.426E+00	−5.338E+00	−9.660E+00	−7.75E+00
		SD	−1.40E+00	6.7972E-02	−5.609E+00	5.8796E-09	0.7118E+00

(*Contd.*)

Table 2 — Comparison of proposed WoOA-TVEC with different algorithms;
(BOA: Butterfly Optimization Algorithm, GA: Genetic Algorithm), Rank: Wilcoxon rank test results (*Contd.*)

Function	Confidence Interval		WoOA-TVEC	WoOA	BOA	GA	PSO
		Rank	1	4	2	5	3
f_{11}	[–5.12, 5.12]	Mean	1.80E-14	2.3864E+01	0	1.6458E+01	1.4453E+02
		SD	1.60E-14	5.5075E+00	0	4.1090E+00	3.7957E+01
		Rank	2	4	1	2	5
f_{12}	[–10, 10]	Mean	9.00E-09	6.0958E+00	0	3.1474E-17	4.4402E-02
		SD	1.20E-10	6.1796E-01	0	3.0784E-16	4.5318E-01
		Rank	3	5	1	2	4
f_{13}	[–100, 100]	Mean	0	8.6622E-16	0	1.6896E-17	0
		SD	0	8.5387E-16	0	1.6896E-16	0
		Rank	1	3	1	2	1
f_{14}	[–10, 10]	Mean	1.00E-06	1.2571E+02	2.8837E+01	3.7872E+01	2.5746E+02
		SD	9.00E-06	8.7373E+01	3.1281E-02	2.5254E+01	3.7311E+02
		Rank	1	4	2	3	5
f_{15}	[–100, 100]	Mean	−8.50E-01	−9.004E-01	−1.000E+00	−1.000E+00	−1.000E+00
		SD	−1.02E+00	2.7310E-01	0	0	0
		Rank	2	3	1	1	1
f_{16}	[–10, 10]	Mean	−9.26E+00	−1.860E+02	−1.867E+02	−1.867E+02	−1.867E+02
		SD	−1.87E+02	5.4273E-10	2.0649E-11	5.5389E-14	2.5708E-13
		Rank	3	2	1	1	1
f_{17}	[–10, 10]	Mean	0	2.3648E-02	0	2.4244E-03	1.2030E+03
		SD	0	4.1886E-02	0	1.0716E-03	5.4485E+02
		Rank	1	3	1	2	4
f_{18}	[–10, 10]	Mean	1.50E-24	1.0006E-01	6.996E-153	4.6662E-02	1.0586E-01
		SD	1.00E-30	6.6005E-01	1.478E-152	1.0895E-02	6.5371E-02
		Rank	1	4	2	3	5
f_{19}	[–10, 10]	Mean	0	1.4218E-01	0	5.4367E-02	7.2800E+01
		SD	0	6.8338E-02	0	0.6187E-02	2.2745E+01
		Rank	1	3	1	2	4
f_{20}	[–500, 500]	Mean	−2.16E+01	−1.059E+04	−2.266E+03	−1.189E+04	−7.570E+03
		SD	−4.17E+02	2.9306E+02	4.5626E+02	2.9530E+02	8.8893E+02
		Rank	1	4	2	5	3
f_{21}	[–10, 10]	Mean	0	1.3204E-11	0	0	0
		SD	0	2.4214E-11	0	0	0
		Rank	1	2	1	1	1
f_{22}	[–2, 2]	Mean	3.00E+00	3.000E+00	3.0000E+00	3.0000E+00	3.0000E+00
		SD	0.00E+00	6.4866E-12	0	0	0
		Rank	1	1	1	1	1
f_{23}	[–10, 10]	Mean	0	1.1932E-04	0	8.388E-104	0
		SD	0	1.3039E-04	0	2.516E-103	0
		Rank	1	3	1	2	1
f_{24}	[–4, 5]	Mean	0	1.5105E+01	0	3.2713E-02	3.3671E+03
		SD	0	1.1057E+01	0	1.1145E-02	9.5201E+02
		Rank	1	3	1	2	4
f_{25}	[0, n]	Mean	1.00E-11	7.1343E-02	2.8400E-02	1.2997E-04	1.9839E-04
		SD	1.00E-11	5.1375E-02	1.3179E-02	1.1326E-04	1.6590E-04
		Rank	1	5	4	2	3
f_{26}	[0, 10]	Mean	−1.02E+01	−1.010E+01	−1.015E+01	−8.900E+00	−1.150E+01
		SD	−5.71E+00	0	0	2.7008E+00	0
		Rank	1	3	4	2	5
f_{27}	[–10, 10]	Mean	0	1.2211E-02	0	3.4256E-03	9.2000E+02
		SD	0	1.2947E-02	0	2.281E-03	8.2704E+02
		Rank	1	3	1	2	4
f_{28}	$[-n^2, n^2$	Mean	−1.50E+03	3.6425E+04	−2.750E+07	−1.035E+03	7.6727E+05
		SD	−2.16E+01	1.9418E+04	5.6521E+07	1.1916E+03	4.0197E-05
		Rank	1	3	5	2	4
f_{29}	[–1, 5]	Mean	−3.81E-01	−3.792E-03	−3.791E-03	−3.791E-03	−3.791E-03

(*Contd.*)

Table 2 — Comparison of proposed WoOA-TVEC with different algorithms;
(BOA: Butterfly Optimization Algorithm, GA: Genetic Algorithm), Rank: Wilcoxon rank test results (*Contd.*)

Function	Confidence Interval		WoOA-TVEC	WoOA	BOA	GA	PSO
		SD	−2.13E-01	5.7115E-18	0	4.5714E-19	0
		Rank	3	2	1	1	1
f_{30}	[−1.2, 1.2]	Mean	0	8.0007E-03	8.0070E-03	9.565E-06	0
		SD	0	9.6124E-03	9.6142E-03	3.0245E-05	0
		Rank	1	3	3	2	1
	Wilcoxon Rank sum		42	89	53	64	90

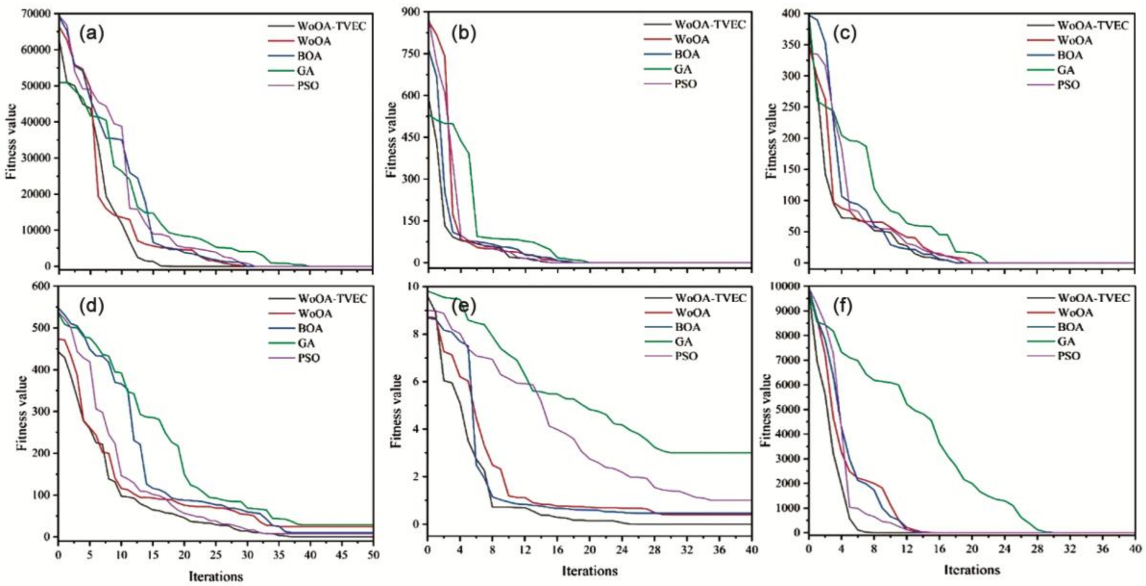

Fig. 4 — Convergence graphs of benchmark functions: (a) F4, (b) F8, (c)F9, (d) F11, (e) F18, (f) F27

functions was utilized, encompassing unimodal functions (to evaluate exploitation capabilities), multimodal functions (to assess exploration strength), and hybrid/composite functions (to test robustness against complex landscapes). These functions are well-established in the literature and are designed to rigorously evaluate an algorithm's adaptability, convergence behavior, and global search efficiency. The comparison indicates that the proposed WoOA-TVEC algorithm performs better in most of the benchmark problems. Additionally, the performance of the proposed algorithm is compared with convergence graphs shown in Fig. 4, where it is observed that the algorithm converges quickly toward the optimal solution.

The proposed WoOA-TVEC algorithm, enhanced with a Time-Varying Exponential Coefficient, effectively distinguishes itself from conventional metaheuristic algorithms such as PSO, GA, and BOA by adaptively balancing exploration and exploitation across the optimization process. The exponential coefficient dynamically modulates the search behavior over time — facilitating broad global exploration during early iterations and intensifying local exploitation in the later stages. This strategic modulation improves convergence speed while reducing the likelihood of premature stagnation in local optima. Empirical evaluations across standard benchmark functions demonstrate that WoOA-TVEC consistently delivers superior convergence, solution quality, and robustness compared to traditional algorithms.

To statistically validate these results, a Wilcoxon rank-sum test was performed to assess the significance of performance differences among the algorithms. The algorithms were ranked based on their test outcomes, with Rank 1 assigned to the algorithm that performed best. In cases where two or more algorithms exhibited statistically indistinguishable performance, equal ranks were assigned. A higher numerical rank corresponds to comparatively poorer performance. This ranking scheme provides an objective and rigorous measure to support the performance claims of the proposed algorithm.

Results and Discussion

When DSM is implemented, the system load is adjusted to change or reschedule power consumption, promoting more efficient use of available resources. In this study, the intermittent nature of solar PV generation is modeled and integrated into the optimization framework as an input to the WoOA-TVEC algorithm. This allows the algorithm to evaluate dynamically how much load demand can be met through renewable sources, then allocate the remaining demand to conventional generators. To achieve the most economical operation of generators, strategies such as ELD and UC are incorporated into the framework. These methods help minimize total generation costs by finding the most cost-effective generator schedule based on hourly changes in net demand (i.e., total load minus PV generation). All essential inputs, including load profiles, PV data, and generator constraints, are supplied to the algorithm before starting the optimization process. This setup enables the algorithm to determine the best load distribution pattern over time, while keeping the total energy consumption within the scheduling period unchanged. As a result, the proposed framework strikes a balance between cost efficiency, renewable resource utilization, and operational viability. The article also shows that applying DSM has improved the overall system stability, as indicated by the L-index in Table 3 below.

The generator scheduling is processed with the help of the ELD program, and it was found that at all times, the 4th and 5th generators were scheduled to operate at their minimum generation for the given load throughout the day. To further reduce the cost, the UC problem is utilized to plan the on and off timings of the generators, as shown in Table 4.

The load data for the IEEE 14-bus system is shown in Fig. 5. It is noted that the load curve is smoother when DSM is applied. To evaluate the effectiveness of the proposed WoOA-TVEC algorithm in DSM optimization, a detailed analysis of the system's hourly load profile was performed. After implementing DSM, the system showed a peak load reduction from 269.227 kW to 247.112 kW, an 8.21% decrease in peak demand. This demonstrates that the algorithm successfully achieved load shifting by redistributing excess demand from peak hours to off-peak periods without changing the total energy usage. A comparative load curve before and after DSM implementation is shown in Fig. 5, illustrating a significantly smoother and flatter load profile post-optimization, which reduces operational stress on generation units and improves grid reliability. The load curve using WoOA-TVEC also visualizes a more optimal temporal distribution of demand compared to the curves generated by other benchmark algorithms, such as PSO and GA. These results confirm the algorithm's capability to perform real-time DSM actions that reduce peak loads while maintaining energy balance and user comfort.

With the help of the WoOA-TVEC algorithm, DSM is applied in the IEEE 14 bus test system and found that the algorithm is efficiently working in reducing the cost and peak load of the system, as shown in Table 5 below. The results were compared with the WoOA and Particle Swarm Optimization (PSO) algorithms since WoOA-TVEC is derived from the WoOA and PSO has gained more popularity among all metaheuristic optimization algorithms. The results show that the proposed WoOA-TVEC algorithm is working better than WoOA and PSO algorithms.

The proposed WoOA-TVEC-based optimization framework, which combines DSM, ELD, UC, and PV systems, notably enhanced both economic and voltage stability in the IEEE 14-bus system. DSM successfully reshaped the load profile, while ELD and UC optimized generation scheduling within cost limits. PV systems were optimally positioned using L-index sensitivity, improving voltage stability. Consequently, the total generation cost decreased from \$169,462 to \$117,986, and the maximum L-index dropped from 0.8757 to 0.5936, representing a 30.35% cost savings and a 32.23% improvement in

Table 3 — L-index values for all buses after implementing DSM and Solar PV

Bus ID	L-index with DSM	L-index with DSM and PV	Bus ID	L-index with DSM	L-index with DSM and PV
Bus-1	0	0	Bus-8	0.5217	0.4962
Bus-1	0	0	Bus-9	0.5074	0.5368
Bus-3	0	0	Bus-10	0.6003	0.6231
Bus-4	0.2481	0.3124	Bus-11	0.6978	0.6419
Bus-5	0.4012	0.4621	Bus-12	0.7709	0.6163
Bus-6	0	0	Bus-13	0.8187	0.6018
Bus-7	0.1659	0.1617	Bus-14	0.8614	0.5826

Table 4 — Generator scheduling following DSM implementation with PV included

Hour of the day	Generator scheduling power output (MVA)					Total load after DSM
	G-1	G-2	G-3	G-4	G-5	
07:00	168.8881	38.1421	16.6798	Off	Off	223.7100
08:00	160.9194	36.8515	16.3184	Off	Off	214.0893
09:00	154.1071	35.7119	15.9993	Off	Off	205.8183
10:00	148.2675	34.6985	15.7156	Off	Off	198.6816
11:00	150.5716	35.0901	15.8252	Off	Off	201.4869
12:00	154.4611	35.7119	15.9993	Off	Off	206.1723
13:00	161.4634	36.8515	16.3184	Off	Off	214.6333
14:00	165.2419	37.3480	16.4574	Off	Off	219.0473
15:00	170.7686	38.1187	16.6732	Off	Off	225.5605
16:00	164.6994	36.8379	16.3146	Off	Off	217.8519
17:00	158.6452	35.6989	15.9957	Off	Off	210.3398
18:00	152.9867	34.6804	15.7105	Off	Off	203.3776
19:00	155.1763	35.0746	15.8209	Off	Off	206.0718
20:00	158.6452	35.6989	15.9957	Off	Off	210.3398
21:00	172.0882	38.1187	16.6732	Off	Off	226.8801
22:00	189.3326	41.2227	17.5424	Off	Off	248.0977
23:00	155.2806	35.0933	15.8261	Off	Off	206.2000
24:00	153.4386	34.7617	15.7333	Off	Off	203.9336
01:00	170.5856	37.8481	16.5975	Off	Off	225.0312
02:00	175.0507	38.6520	16.8226	Off	Off	230.5253
03:00	175.0507	38.6520	16.8226	Off	Off	230.5253
04:00	170.5331	37.8482	16.5975	Off	Off	224.9788
05:00	171.4502	38.0192	16.6454	Off	Off	226.1148
06:00	150.0169	34.5415	15.6716	Off	Off	200.2300

Table 5 — Performance evaluation related to cost and peak load

Algorithm		Cost ($)	% Reduction	Peak load (MVA)	% Reduction
Before DSM		169462	—	269.227	—
	Best	131421	22.44	249.367	7.37
PSO	Worst	136862	19.23	257.814	4.23
	Average	132651	21.72	251.362	6.63
	Best	117125	30.88	246.325	8.50
WoOA	Worst	119364	29.56	251.482	6.63
	Average	118333	30.17	248.097	7.84
	Best	116125	31.47	246.362	8.49
WoOA-TVEC	Worst	118254	30.21	249.213	7.43
	Average	117986	30.37	247.112	8.21

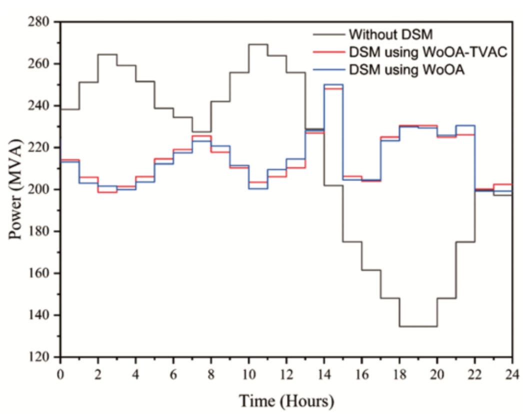

Fig. 5 — Load data following the application of DSM

voltage stability. As shown in Table 5, WoOA-TVEC outperformed other algorithms across best, worst, and average performance over 30 runs. The algorithm was executed in MATLAB on an Intel i9 processor. The convergence pattern in Fig. 6 demonstrates faster and more stable convergence than benchmark methods, confirming the robustness and effectiveness of the proposed approach.

DSM is crucial to improving the efficiency, reliability, and cost-effectiveness of electricity systems. DSM methods include load shifting, peak shifting, and energy saving, all of which try to modify consumer demand patterns. When applied to the IEEE

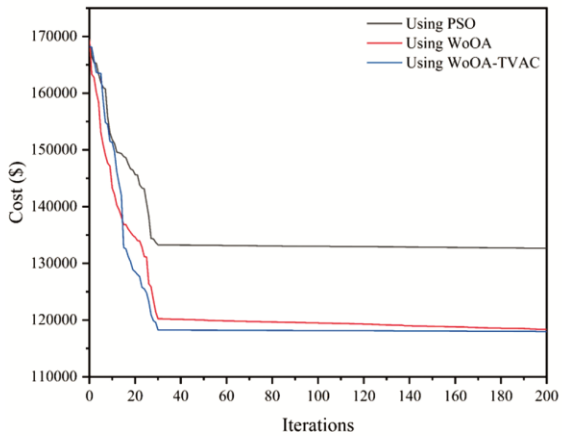

Fig. 6 — Convergence graph

14-bus system, a standard benchmark for small to medium-sized power networks, DSM techniques are evaluated for their impact on load flow, stability, and economic operation. DSM contributes to ELD by optimizing generating costs while ensuring system load and operational restrictions are satisfied. DSM can lower peak loads and increase generating cost efficiency by changing demand patterns. Time-of-Use (TOU) pricing, obtained from the ELD application, encourages customers to reduce their usage during peak hours. These methods not only lower generation costs by using less expensive producing units, but they also improve the reliability of the system by better matching demand to available supply. For UC, DSM is crucial in deciding the on/off state of generation units to save operational expenses during a specified schedule period. DSM methods can be used as decision variables in UC models. These technologies enable flexible demand to match the availability of renewable energy sources, decreasing reliance on expensive peaking units. The advantages of this integration include increased operational flexibility and lower fuel costs through the optimal use of renewable and efficient generating units. When simulating DSM in the IEEE 14-bus system, strategies like load shifting and demand response programs are applied to individual buses. These solutions assist in shifting loads from peak to off-peak hours, balancing demand and supply. By modeling consumer engagement and load redistribution, the efficacy of DSM measures can be assessed and optimized. Despite its merits, deploying DSM in systems such as the IEEE 14-bus paradigm presents hurdles. Due to the unpredictability of demand, accurate modeling of consumer behavior and participation in DSM programs is crucial. Furthermore, system restrictions such as voltage limits, line capacity, and generator limits must be respected throughout DSM simulations. Economic consequences must also be carefully considered to balance cost reductions with the expenses of implementing DSM techniques. DSM in the IEEE 14-bus system is predicted to result in increased cost efficiency through optimal generating schedules, greater system stability, and lower risks of congestion or outages. Furthermore, DSM promotes the integration of renewable energy by matching demand with intermittent supply, thus boosting sustainability. These advantages underscore the need to integrate DSM techniques into ELD and UC challenges, thereby creating a more robust and cost-effective power system.

Conclusions

This study presents a novel energy optimization framework that integrates DSM with the WoOA-TVEC algorithm, designed to address operational and environmental challenges in power systems. Incorporating a Time-Varying Exponential Coefficient enhances the algorithm’s ability to balance exploration and exploitation, improving optimization results. The method effectively addresses ELD while considering economic factors and utilizes L-index-based analysis for the strategic placement of PV systems. The approach demonstrates significant potential for reducing operational costs by 30.35%, facilitating the effective integration of renewable energy with a penetration of 37.45% by reducing the system's peak load demand by 8.21%, and enhancing overall system performance. Its performance was thoroughly tested using statistical metrics such as mean and standard deviation across 30 independent simulations. A Wilcoxon rank-sum test was used for objective comparison, and convergence behavior was analyzed using selected benchmark problems. Although demonstrated on a standard test case, the method is scalable and suitable for larger, more complex smart grid systems with high penetration of renewable energy. This approach provides valuable support for the sustainable, stable, and cost-effective operation of energy systems in smart grid environments, particularly as renewable energy adoption and urban energy demands continue to increase.

References

1 Shewale A, Mokhade A, Lipare A & Bokde N D, Efficient techniques for residential appliances scheduling in smart homes for energy management using multiple knapsack problem, *Arab J Sci Eng*, **49(3)** (2024) 3793–3813.

2 Dey B, Basak S & Bhattacharyya B, Demand-side-management-based bi-level intelligent optimal approach for cost-centric energy management of a microgrid system, *Arab J Sci Eng*, **48(5)** (2023) 6819–6830.

3 Heydari A H, Khoshkhoo R H, Zahedi R & Noorollahi Y, Demand side management optimization and energy labeling of multi-purpose buildings, *J Build Eng*, **88** (2024) 109–143.

4 Eltamaly A M, A novel energy storage and demand side management for entire green smart grid system for NEOM city in Saudi Arabia, *Energy Storage*, **6(1)** (2024) e515.

5 Ireshika M A S & Kepplinger P, Uncertainties in model predictive control for decentralized autonomous demand side management of electric vehicles, *J Energy Storage*, **83** (2024) 110–194.

6 Dawoud S M, Elkadeem M R, Abido M A, Atiya E G, Lin X, Alzahrani A S & Kotb K M, An integrated approach for cost- and emission optimal planning of coastal microgrid with demand-side management, *Sustain Cities Soc*, **101** (2024) 105–149.

7 Bustos R, Marin G, Navas Fonseca A, Reyes Chamorro L & Saez D, Hierarchical energy management system for multi-microgrid coordination with demand-side management, *Appl Energy*, **342** (2023) 121–145.

8 Alhasnawi B N, Jasim B H, Alhasnawi A N, Hussain F F K, Homod R Z, Hasan H A & Sedhom B E, A novel efficient energy optimization in smart urban buildings based on optimal demand side management, *Energy Strateg Rev*, **54** (2024) 101–461.

9 Yuan J, Gang W, Xiao F, Zhang C & Zhang Y, Two-level collaborative demand-side management for regional distributed energy system considering carbon emission quotas, *J Clean Prod,* **434** (2024) 140–095.

10 Nagarajan K, Rajagopalan A, Bajaj M, Sitharthan R, Dost Mohammadi S A & Blazek V, Optimizing dynamic economic dispatch through an enhanced Cheetah-inspired algorithm for integrated renewable energy and demand-side management, *Sci Rep*, **14(1)** (2024) 3091.

11 Basak S & Bhattacharyya B, Optimal scheduling in demand-side management-based grid-connected microgrid system by hybrid optimization approach considering diverse wind profiles, *ISA Trans*, **139** (2023) 357–375.

12 Zhao F, Li Z, Wang D & Ma T, Peer-to-peer energy sharing with demand-side management for fair revenue distribution and stable grid interaction in the photovoltaic community, *J Clean Prod*, **383** (2023) 135–271.

13 Liu Y, Li H, Zhu J, Lin Y & Lei W, Multi-objective optimal scheduling of household appliances for demand side management using a hybrid heuristic algorithm, *Energy*, **262** (2023) 125–460.

14 Asgharzadeh F, Tabar V S & Ghassemzadeh S, Stochastic bi-level allocation of electric vehicle charging stations in the presence of wind turbines, crypto-currency loads and demand side management, *Electr Power Syst Res*, **220** (2023) 109–383.

15 Roshan A & Ganga D, Intelligent categorization and interactive mechanism for smart demand side management of residential consumers, *Sustain Energy Grids Netw*, **37** (2024) 101–255.

16 Singh S, Saket R K, Gupta A R & Tripathi J M, Impact analysis of demand side management for maintaining the voltage profile of distribution system, *J Inst Eng India Sers B*, (2024) 1–17.

17 Praveen M & Gadi V S K R, Hybrid emperor penguin glowworm swarm optimiser for techno-economical optimisation with demand side management in microgrid using multi-objective function, *Int J Ambient Energy*, **45(1)** (2024) 277–302.

18 Karimi H & Jadid S, Multi-layer energy management of smart integrated-energy microgrid systems considering generation and demand-side flexibility, *Appl Energy*, **339** (2023) 120–984.

19 Kumar S, Kumar A & Sharma N K, A novel method to investigate voltage stability of IEEE-14 bus wind integrated system using PSAT, *Front Energy*, **14(2)**(2020) 410–418.

20 Misra S, Panigrahi P K, Ghosh S & Dey B, A metaheuristic approach to compare different combined economic emission dispatch methods involving load shifting policy, *Environ Dev Sustain*, (2024) 1–23.

21 Modarresi J, Gholipour E & Khodabakhshian A, A comprehensive review of the voltage stability indices, *Renew Sustain Energy Rev*, **63** (2016) 1–12.

22 India Smart Grid Forum, *Smart Grid Handbook for Regulators and Policymakers*, **vol. 2**, p. 29.12, 2023. [Online]. Available: https://indiasmartgrid.org/isgf/public/banner_img/1696483578oM1Iim1MuH412bOdmctUBEHxndnT3Zmcud8wRLwb.pdf#page=29.12

23 Lekshmi Nair K B, Haripriya M R & Shereef R M, Improvement of load factor in power distribution networks using electric vehicles, *Electr Eng*, (2024), 1–12.

24 Hamadneh T, Batiha B, Alsayyed O, Werner F, Monrazeri Z, Dehghani M & Eguchi K, Using the novel wolverine optimization algorithm for solving engineering applications, *CMES-Comput Model Eng Sci*, **141(3)** (2024).

25 Arora S & Singh S, Butterfly optimization algorithm: a novel approach for global optimization, *Soft Comput,* **23** (2019) 715–734.